

Space Weather

RESEARCH ARTICLE

10.1029/2018SW002003

Key Points:

- Physics-based frameworks are one way to assess the economic impact of space weather for policy and risk management
- A methodology based on substorms, and including forecast quality, is proposed to model geomagnetic storm impact
- The 1-in-10-, 1-in-30-, and 1-in-100-year scenarios are developed, and example calculations of economic impact are presented

Supporting Information:

- Supporting Information S1
- Table S1
- Table S2
- Table S3

Correspondence to:

J. P. Eastwood,
jonathan.eastwood@imperial.ac.uk

Citation:

Eastwood, J. P., Hapgood, M. A., Biffis, E., Benedetti, D., Bisi, M. M., Green, L., et al. (2018). Quantifying the economic value of space weather forecasting for power grids: An exploratory study. *Space Weather*, 16, 2052–2067. <https://doi.org/10.1029/2018SW002003>

Received 4 JUL 2018

Accepted 15 NOV 2018

Accepted article online 28 NOV 2018

Published online 20 DEC 2018

Quantifying the Economic Value of Space Weather Forecasting for Power Grids: An Exploratory Study

J. P. Eastwood¹ , M. A. Hapgood² , E. Biffis³, D. Benedetti³ , M. M. Bisi² , L. Green⁴, R. D. Bentley⁴, and C. Burnett⁵

¹The Blackett Laboratory, Imperial College London, London, UK, ²RAL Space, STFC Rutherford Appleton Laboratory, Didcot, UK, ³Department of Finance, Imperial College Business School, Imperial College London, London, UK, ⁴Mullard Space Science Laboratory, University College London, Dorking, UK, ⁵Space Weather Programme, Met Office, Exeter, UK

Abstract An accurate understanding of space weather socioeconomic impact is fundamental to the development of appropriate operational services, forecasting capabilities, and mitigation strategies. One way to approach this problem is by developing physics-based models and frameworks that can lead to a bottom-up estimate of risk and likely impact. Here we describe the development of a new framework to assess the economic impact of space weather on power distribution networks and the supply of electricity. In particular, we focus on the phenomenon of the geomagnetic substorm, which is relatively localized in time and space, and occurs multiple times with varying severity during a geomagnetic storm. The framework uses the *AE* index to characterize substorm severity, and the impact of the substorm is modulated by the resilience of the power grid and the nature of available forecast. Possible scenarios for substorm sequences during a 1-in-10-, a 1-in-30-, and a 1-in-100-year geomagnetic storm events are generated based on the 2003, 1989, and 1859 geomagnetic storms. Economic impact, including international spill over, can then be calculated using standard techniques, based on the duration and the geographical footprint of the power outage. Illustrative calculations are made for the European sector, for a variety of forecast and resilience scenarios. However, currently available data are highly regionally inhomogeneous, frustrating attempts to define an overall global economic impact at the present time.

1. Introduction

The need for a stable, reliable supply of electricity lies at the heart of modern society. The primary terrestrial risk attached to space weather is therefore its impact on conducting ground infrastructure, specifically power distribution networks (e.g., Cannon et al., 2013; Eastwood, Biffis, et al., 2017; Hapgood, 2010; Lloyd's, 2013; Oughton et al., 2017; Schrijver et al., 2015). The primacy of security of power supply is recognized, for example, by the fact that several major meetings have been organized on this subject in the past few years (e.g., Showstack, 2011). Furthermore, space weather is now included in lists of events and phenomena that may have a worldwide economic impact as documented by the Organisation for Economic Co-operation and Development and the World Economic Forum (Howell, 2013; Organisation for Economic Co-operation and Development, 2011).

Although space weather generates a multitude of impacts and risk factors, geomagnetic activity is by far the most relevant for power distribution systems. The Earth's magnetic field forms the magnetosphere, whose dynamics are strongly driven by the solar wind (e.g., Eastwood, Nakamura, et al., 2017). This mainly depends on the strength and orientation of the interplanetary magnetic field and the solar wind speed. Magnetic reconnection allows energy and solar wind plasma to enter the magnetosphere on the dayside; energy is stored and explosively released on the nightside. The elemental response of the magnetosphere is the geomagnetic substorm, which occurs periodically in response to intervals of southward interplanetary magnetic field in the solar wind and notably produces vivid auroral displays at high latitudes. Strong prolonged driving of the magnetosphere can lead to the development of a geomagnetic storm. Within geomagnetic storm intervals, power grids are affected by ground induced currents (GICs), driven by storm-generated geoelectric fields, which are induced by rapidly changing magnetic fields at and within the Earth's surface (dB/dt ; e.g., Viljanen et al., 2006).

GICs may impact power grids in three ways (e.g., Cannon et al., 2013, and references therein): They may damage the physical infrastructure (specifically transformers, although this also depends on the

transformer design), they may introduce voltage instability, which could lead to a blackout without damaging the infrastructure, and they may interfere with the operation of protection systems and fault detection. The severity of a GIC impact is often measured or monitored according to the local rate of change of the horizontal geomagnetic field dB/dt , on time scales of seconds to minutes (Beamish et al., 2002). In the United Kingdom, passing the threshold of 500 nT/min would constitute a GIC impact with possible adverse impact (Cannon et al., 2013; Erinmez et al., 2002). A 1-in-100-year event may exhibit changing magnetic fields as large as 5,000 nT/min (Natural Environment Research Council, 2010; Thomson et al., 2011).

There are many documented impacts of space weather on power grids. For example, in the United Kingdom two transformers were damaged during the 13 March 1989 storm (Erinmez et al., 2002; Smith, 1990). Thomson et al. (2005) examined the impact on the Scottish power grid of the 2003 storms and described how the models presented in the paper were being used to monitor, warn, and analyze the properties of GICs. Distortion of the magnetizing current causing harmonics, which interfere and possibly trigger protective relays, has been detected in the UK national grid on 14 July 1982, 13–14 March 1989, 19–20 October 1989, and 8 November 1991 (Cannon et al., 2013).

The impact on continental Europe has been examined at regional level particularly focusing on high latitudes, for example, Finland (Juusola et al., 2015; Pirjola et al., 2005). The impact of the 2003 storms on the Swedish high voltage power transmission system is reported by Pulkkinen et al. (2005). In this case, a 90-min blackout left 50,000 customers without power in southern Sweden. This blackout arose because of protective relays being erroneously triggered (Cannon et al., 2013). GICs have also been reported at midlatitudes, for example, in Spain and Europe more generally as part of the FP7 EURISGIC project (Torta et al., 2012; Viljanen, 2011).

In North America, the impact of the 1989 geomagnetic storm on the Quebec power grid and its failure is described in detail by Bolduc (2002). This blackout arose also from the triggering of protective relays (Cannon et al., 2013). A detailed technical assessment by Metatech Corp. examining the wider impact of geomagnetic storms on the North American power grid (Kappenman, 2010) includes a specific assessment of the 1989 event. In addition, an analysis of power grid performance data by Forbes and St Cyr (2012) examined whether power system reliability was challenged regionally in the United States during solar cycle 23 and concludes that “geomagnetic activity can significantly increase the likelihood that the system operator will dispatch generating units based on system stability considerations rather than economic merit.” Adverse impacts on the U.S. power grid between 1992 and 2010 have also been analyzed by Schrijver and Mitchell (2013). They conclude that 4% of the disturbances reported to the U.S. Department of Energy are attributable to strong geomagnetic activity. A further study by Schrijver et al. (2014) suggests that space weather-induced variations in the quality of electric power lead to around 500 insurance claims per year in the United States for equipment malfunctions due to power supply problems.

Although the majority of the literature focuses on North America and Europe, other regions have been investigated. The impact on South Africa has been studied by a number of authors (e.g., Lotz & Cilliers, 2015, and references therein; Matandirotya et al., 2015). Of particular importance here is the work by Gaunt and Coetzee (2007). The impact of GICs in Japan has been studied, for example, by Watari (2015). Similarly, GIC impact in China has been reported by Wang et al. (2015). The impact of GICs on the Brazilian power system has been reported by Trivedi et al. (2007), based on measurements since early 2004 (motivated in part by the impact in South Africa of the 2003 geomagnetic storms).

The economic impact of any hazard is a function of the (i) spatial and temporal extent of the hazard, (ii) the vulnerability of the technologies/infrastructures susceptible to failure, (iii) the degree of mitigation (backup generation), and (iv) and input production and consumption options available to firms and consumers. It has been argued that a 1-in-100-year event (i.e., Carrington class, such as the 1859 space weather event; Stewart, 1861) could lead to catastrophic impact, with damage to transformers taking a considerable length of time (years) to recover from, and a consequent economic impact in the trillions of dollars range because of the lack of power for a very prolonged period of time (Kappenman, 2010). In such a scenario, it has been calculated that the worldwide direct and indirect losses from a Quebec-like space weather event whose outage is extended to 1 year would range “from \$2.4 trillion - \$3.4 trillion over a year” (Schulte in den Baeumen et al., 2014). In contrast, the 2012 North American Electric Reliability Corporation report (Natural Environment Research Council, 2012) finds that the more likely impact is system collapse due to voltage instability. In this case the outage would be measured in hours to days, rather than months. This is mirrored in the opinion of

the UK impact report by Cannon et al. (2013) who conclude that the current worst-case estimate for the impact of a Carrington-class event on the UK power grid is for some local blackouts due to voltage instability lasting a few hours and damage to *super grid* transformers (an approximate estimate of around 6 in England and Wales and 7 in Scotland). More recently, Gaunt (2014) has shown that there are still considerable uncertainties in our understanding of the potential of GIC to damage transformers. Thus, we consider short-term blackouts as a clear lower bound for the grid impacts that we consider here. Such blackouts lasting even a few days can have a considerable economic impact. For example, the economic impact of the 14 August 2003 northeast blackout was estimated to be \$4 to \$10 billion (U.S.-Canada Power System Outage Task Force, 2006), with a more refined estimate using input-output (IO) modeling of \$6.53 billion (Anderson et al., 2007). While this blackout was due to bad weather and a failure to control vegetation near power lines, it provides a good way to cross-calibrate estimates of space weather economic impacts.

One example of such a study was carried out by ABT associates on behalf of NOAA and concluded that a severe space weather event might lead to a loss of power over a large region of the United States for up to 9 hr, costing U.S. consumers of electricity up to \$20bn (ABT Associates, 2017). A more detailed study of the U.S. power grid was carried out by the Cambridge Centre for Risk Studies (Oughton et al., 2016; see also Oughton et al., 2017). This model indicates a loss of U.S. gross domestic product between \$135 and \$610 billion over a 5-year period following the space weather event, with the worst affected states being Illinois and New York. It also indicates significant knock-on impacts to the global economy with China, Canada, and Mexico being worst affected (as they are the U.S.' largest trading partners) but also significant impacts on the United Kingdom, Japan, and Germany.

A recent study (https://www.esa.int/About_Us/Business_with_ESA/GSEF/A_cost-benefit_analysis_of_the_SSA_programme) commissioned by the European Space Agency's Space Situational Awareness program performed by PricewaterhouseCoopers provides a cost-benefit analysis of the Space Weather program (European Space Agency, ESA, 2016). The *best educated estimate* of the impact is a blackout affecting three cities for three days in the case of a G5-G5+ event. By modeling this impact on three *average* European cities (i.e., geographically nonspecific) and assuming that the current space weather monitoring capability is available, the cost is found to be €5.771 billion. The impact of morbidity and power infrastructure damage is also accounted for. Oughton et al. (2018) explore the specific impact of severe space weather on the UK, tensioned against forecast quality. For a 1-in-100-year event, they find gross domestic product loss as high as £15.9bn, reducing to £2.9bn with current forecasting and further reduced to £0.9bn in a scenario with improved forecasting. Finally, we also note the very recent publication by Oughton (2018) of a meta-review on the economic impact literature produced to date.

As a matter of public policy, there is therefore considerable interest in understanding the economic risk of space weather, and therefore, an econometric framework is required that is strongly grounded in the underlying physical phenomena. Furthermore, to be useful as a policy tool, it is also necessary to understand the feedback of investment to address the space weather risk. The purpose of this article is to report the development of a new econometric framework developed from the ground up. Two key aspects are as follows. The first is to use a substorm-based approach, rather than *Dst* or *Kp*. The second is to characterize the impact of improved situational awareness, manifested as a reduction in the impact footprint. The approach is designed to be modular and scalable, with flexibility built in at several levels, allowing for a range of forecast outcomes based on adjusting model parameters.

The work is organized as follows. Our methodology, which is based on the construction of substorm time series, is described in section 2. The impact of a particular substorm on a particular geographic region is a function of the substorm severity, the resilience of the network (i.e., its ability to recover from an external disruptive event; Henry & Emmanuel Ramirez-Marquez, 2012; Pant et al., 2014), and the quality of the forecast. This leads to a projected outage impact. Evidently, the precise decisions used here are, to some extent, subjective, but we emphasize the importance of the framework in allowing different parameters to be adjusted leading to a range of forecasted impacts, which furthermore can be explored by recategorizing substorms, networks, and forecast quality. Section 3 then uses historic data from the 1989, 2003, and 1859 storms to construct 1-in-10-, 1-in-30-, and 1-in-100-year scenarios. Section 4 examines how these data can be translated into a calculation of economic impact and focuses on the building block of the model, an individual substorm, here modeled over western Europe. Finally, section 5 provides a discussion of the current obstacles to the full implementation of the framework model and proposals for future work.

2. Methodology

One conclusion to be drawn from the documented impact of space weather is that this does not simply depend on geophysical characteristics. It also depends on the properties of the network (its resilience) and the quality of the available forecast. For example, the National Grid in the United Kingdom is particularly aware of the impact on large super grid transformers, which reduce the voltage from the transmission system to the local distribution networks (Cannon et al., 2013). Consequently, models should account for both the physical driver and the system response. In their study of economic impact, Oughton et al. (2016) defined an innovative parameterization of grid impacts that has allowed the authors to explore a range of possibilities, reflecting different expert views on grid susceptibility. In particular, it included lower and higher estimates of the level of disruption and damage to critical grid hardware such as transformers, as well as a range of recovery times. It also resolves impacts to the level of individual U.S. states taking account of geomagnetic latitude, ground conductivity, and the number of transformers in each state.

In developing the present physics-based framework that treats substorms and GICs as the primary risk to power grids, we propose that the impact depends on three key factors: (1) the size of the physical driver, (2) the resilience of the grid, and (3) the quality of the forecast. The first two factors are self-evident and are discussed in sections 2.1 and 2.2 below. The final factor is included to account for the reasonable assumption that the quality of the space weather information available to a grid operator will make a material difference to their operational response and thus reduce the size of the impact. We consider three levels of forecast quality: *no forecast*, in which there is no L1 coronagraph or solar wind data; *current forecast*, in which there are the currently available assets and forecasts; and *improved forecast*, where an augmented space-based monitoring system with spacecraft at the Sun-Earth L1 and L5 Lagrange points is available. This is discussed further in section 2.3, and the mapping of the physical driver to its impact is discussed in section 2.4.

2.1. Quantification of the Physical Driver

Although the precise relationship between substorms and storms remains unclear and a topic of active research, most operational space weather services focus on the incidence of storms, and characterize their severity on an intensity scale from 1 (*weakest*) to 5 (*strongest*); this is derived from the K_p index ($K_{p_{\max}} = 9$; Bartels et al., 1939). However, since K_p captures the severity of the global perturbation to the quiet magnetic field, it is not directly useful for understanding the most important societal impact—the production of GICs that may affect power grids. Consequently, a simple probabilistic statement that a G5 storm has a certain chance of causing a blackout does not necessarily contain the essential physics that controls the underlying behavior. A more appropriate index is arguably the AE index, used to characterize the ground magnetic field perturbation caused by substorms through the currents generated by the aurora (Davis & Sugiura, 1966). Substorm related fluctuations have been identified as the drivers of major impacts (Fiori et al., 2014; Villiers et al., 2017), not least the events of 1989 and 2003 described above, as well as earlier events in 1982 (United Kingdom/Sweden) and 1972 (United States; Lanzerotti, 1992). While this is not yet used in the operational domain, it is widely used scientifically, and data are easily available. It also has the advantage of being compatible with regional forecasting, which is a goal of agencies currently tasked with forecasting space weather.

Although GICs are mainly created at high latitudes by the electrical ionospheric currents caused by substorms and are regionally located on scales of 500–1,000 km (Ngwira et al., 2013; Pulkkinen et al., 2015), they can be produced by other mechanisms. We note that (a) the initial compression of the magnetosphere by interplanetary shocks can also drive GICs both in equatorial regions (Carter et al., 2015) and at middle and low latitudes (Kappenman, 2003; Marshall et al., 2012) and (b) changes in the ring current can drive GICs in low-latitude regions (Gaunt & Coetzee, 2007). Consequently, by constructing a framework based on substorms, it will be possible, as our understanding progresses, to fit this into the wider understanding of geomagnetic storm activity in a robust and sensible way, alongside other storm effects. Here we describe the intensity of substorms qualitatively: very intense ($AE > 1,900$ nT), intense ($1,500 < AE < 1,900$ nT), high ($1,200 < AE < 1,500$ nT), and moderate ($500 < AE < 1,200$ nT). Note that we do not consider events with $AE < 500$ nT. The motivation for using these categories is discussed in section 2.4 below.

2.2. Grid Resilience

The second dimension is the resilience of the network itself to space weather. In Table 1 we provide an initial assessment of a possible characterization of grid resilience. This represents the simplest possible characterization at a very coarse level—is the grid resilience high or low? This depends on (a) the geographic

Table 1
A Preliminary Possible Assessment of Power Grid Resilience to Space Weather by Region

| Region | Country | Possible Rationale for assessment | Possible grid resilience assessment |
|-----------------------------|-----------------------|--|-------------------------------------|
| Australasia | Australia (main grid) | Applies to tree structure in main grid in east and south of Australia, particularly parts in Victoria, South Australia, and Tasmania, which are assessed to have significant vulnerabilities. Neglect separate grids and local generation in Western Australia and Northern Territory. | Low |
| | New Zealand | Good engagement from system operator, for example, as in measures taken during the Halloween 2003 storm and following space weather damage to a transformer in 2001. | High |
| North America | Canada (Quebec) | Highly engaged system operator. | High |
| | United States | Highly fragmented grid operation. | Low |
| Asia | China | Extensive modern grid with many very high voltage lines. Large GICs reported in some regions, even on southern coast. Scientific publications indicate very high interest in research/power engineering community. | Low (at the moment) |
| | India | Highly stressed system. Conventional geomagnetic storm effects may be rare at low latitude of India, but these effects would have major impact on those rare occasions. Sudden impulse effects due to arrival of a large fast CME would affect India if that arrival was near local noon in India. | Low |
| | Japan | Historically thought to be at low risk of GIC due to low geomagnetic latitude but was formally recognized as significant risk in 2015 and subject of ongoing studies. | Low (at the moment) |
| | Russia | Much of the grid has a tree-like structure, and some parts are at relatively high latitudes. | Low |
| | Finland | High awareness in national community; also choice of transformer designs has greatly reduced risks. | High |
| | Norway | Extensive local power generation from hydro. | High |
| Scandinavia | Sweden | High awareness in national community. | High |
| | France | The mesh structure of the French grid is a significant technical advantage, but perceived poor engagement of operators remains concerning. | Low |
| Western Europe ^a | Belgium | Significant dependence on France. | Low |
| | Germany | Good mesh structure should give high resilience, but significant dependence on France, especially when renewable power is low (nighttime and lack of wind). | Low |
| | Netherlands | Interconnected with Germany. | Low |
| | Denmark | Strongly interconnected with Germany. | Low |
| | Italy | Significant dependence on France. | Low |
| | Switzerland | Substantial resources (nuclear and hydro), some dependence on France. | High |
| | United Kingdom (GB) | Good mesh structure in grid; high engagement from system operator and government. | High |
| | Ireland (ROI/NI) | Growing engagement from system operator and governments. | High |
| | South Africa | Highly stressed system; extensive tree structure in grid. | Low |
| | | | |

Note. GIC = ground induced current; CME = coronal mass ejection.

^aNote that there is significant evidence that grid problems can trigger cascade failures across mainland of western Europe.

location of the network, (b) the structure of the network, (c) the typical stress on the network, (d) any use of transformers and other equipment that is more space weather resilient and (e) the perceived engagement from the system operator.

2.3. Forecast Quality

The three forecast scenarios (no forecast/current forecast/improved forecast) are defined as follows:

- *No forecast available.* This reflects a position where existing satellite observing systems are not replaced prior to the end of their operational life expectancy or at the end of the scientific mission for which they were originally intended.

Table 2
Impact Table Based on Severity of Substorm and Grid Resilience, As Well As Level of Forecast

| Substorm strength | No forecast Grid resilience | |
|-------------------|--|---|
| | Low | High |
| Very intense | Widespread power outage (50%) recovered in 72 hr; some areas (5%) without power for 6 weeks; system capacity reduced by 20% recovered in 2 years | Limited power outage (20%) recovered in 48 hr; some areas (5%) without power for 2 weeks; system capacity reduced by 8% recovered in 5 months |
| Intense | Limited power outage (10%) recovered in 72 hr; some areas (1%) without power for 4 weeks; system capacity reduced by 4% recovered in 5 months | Limited power outage (4%) recovered in 48 hr; some areas ($\leq 1\%$) without power for ≤ 2 weeks |
| High | Limited power outage (2%) recovered in 48 hr | None |
| Moderate | None | None |
| Substorm strength | Current forecast Grid resilience | |
| | Low | High |
| Very intense | Widespread power outage (50%) recovered in 24 hr; some areas (5%) without power for 2 weeks; system capacity reduced by 20% recovered in 2 years | Limited power outage (10%) recovered in 24 hr; some areas (1%) without power for 2 weeks; system capacity reduced by 4% recovered in 5 months |
| Intense | Limited power outage (10%) recovered in 24 hr; some areas (1%) without power for 2 weeks; system capacity reduced by 4% recovered in 5 months | Limited power outage (2%) recovered in 24 hr |
| High | Limited power outage (2%) recovered in 24 hr | None |
| Moderate | None | None |
| Substorm strength | Improved forecast Grid resilience | |
| | Low | High |
| Very intense | Widespread power outage (20%) recovered in 24 hr; some areas (5%) without power for 2 weeks; system capacity reduced by 10% recovered in 2 years | Limited power outage (10%) recovered in 12 hr; some areas (1%) without power for 2 weeks; system capacity reduced by 2% recovered in 5 months |
| Intense | Limited power outage (4%) recovered in 24 hr; some areas (1%) without power for 2 weeks; system capacity reduced by 2% recovered in 5 months | Limited power outage (1%) recovered in 12 hr |
| High | None | None |
| Moderate | None | None |

- *The current level of forecast.* Currently, forecasting relies on data from multiple satellites including the Deep Space Climate Observatory, the Solar and Heliospheric Observatory, and the Advanced Composition Explorer all located in the vicinity of the first Sun-Earth Lagrange point (L1), and the Geostationary Operational Environmental Satellites and Solar Dynamic Observatory in Earth orbit.
- *Improved level of forecasting.* Reflecting the standard that could be achieved if the current observation satellites were supplemented by satellites off the Sun-Earth line, as demonstrated by the Solar TErrestrial RElations Observatory mission, for example, at the fourth and fifth Sun-Earth Lagrange points (L4 and/or L5; e.g., ESA, 2016). Although there have been projects to address in situ measurements of the solar wind from sub-L1 (Eastwood et al., 2015), any realistic, near-term, improved, operational system will rely on measurements from L1 and L5. Even though this improved system would not offer a specific improvement in the knowledge of the magnetic field orientation upstream of the Earth, the value of imaging the Sun away from the Sun-Earth line and the knowledge of the solar wind conditions provide actionable information that end users will use to maximize preparedness.

2.4. Mapping the Physical Driver to the Impact

The impact severity depends on substorm strength, power grid resilience, and forecast quality. The severity and the resilience combine to set the level of the overall impact. The level of the available forecast may

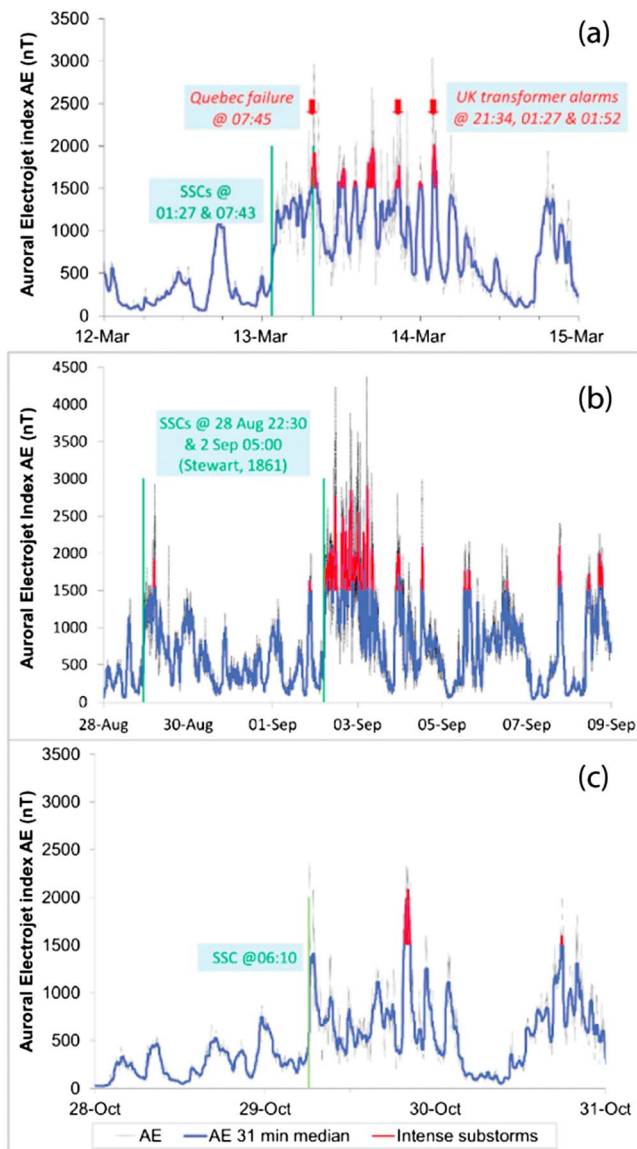


Figure 1. (a) Time series of the AE index during the 1989 storms (gray), with a 31-min running median trace overlaid (blue). Intervals of intense substorms ($AE > 1,500$ nT) are shown in blue. The times of the sudden storm commencement are shown as well as historical impacts. (b) Proposed time series for a Carrington-like 1-in-100-year event, derived from the 1989 observations. (c) Proposed AE time series for a 1-in-10-year event corresponding to the AE index for the October 2003 storm, adjusted as described in the text. SSC = sudden storm commencement.

change both the level of the impact and its duration. Table 2 summarizes the estimated impact severity based on these three factors. Here the impact table is informed by the analysis in the Royal Academy of Engineering report (Cannon et al., 2013).

The calibration of qualitative substorm intensity and impact is defined by reports of major GIC impacts. Very intense substorms caused the impacts experienced in the United Kingdom and Quebec during the March 1989 storm (see Figure 1a). Another very intense substorm early on 14 July 1982 (not shown) caused loss of power in parts of Scotland (Beamish et al., 2002) and rail signal disruption (green lights turned red) in Sweden (Wik et al., 2009). An intense substorm just after 21:00 UT on 13 March 1989 (Figure 1a) also caused an alarm on a UK transformer, while an intense substorm around 20:00 UT on 30 October 2003 (Figure 1c) caused a loss of power in Malmö in Sweden (Wik et al., 2009). These events give confidence that the substorm classes of intense and very intense indicate a potential for disruptive levels of GIC in power grids and rail systems, especially at upper middle latitudes (45° – 60°). This approach is also consistent with the analysis in the Royal Academy of Engineering report of space weather impacts on engineered systems (Cannon et al., 2013). The lower end of our scale of substorm classes and their impacts is then set by scaling down the impacts from the higher end of the scale. For high resilience power grids this scaling down is simply that we expect zero impact from the lower substorm classes. For less resilient grids, our scaling down allows for minor impacts from events in our third substorm class (high). Here resilience arises from several factors including (a) the hardening of grid assets, such as transformers, to withstand substantial GICs; and (b) good awareness of the risk, so that the grid operator is ready to ensure grid stability (e.g., through provision of additional reactive power) during a severe space weather event.

The impact severity has been scaled so that this declines with increasing forecast capability. A key assumption we make is that better forecasts improve the speed of recovery, since the recovery management process can be better prepared for (Cabinet Office, 2015). Much of the economic impact arises from the disruption of productive activities over the recovery period, rather than from the immediate impact of the space weather event (a substorm in our framework). Thus, our framework provides a scaling of recovery times that allows us to compare different forecast schemes. For the present study we have assigned what we consider to be realistic recovery times, based, for example, on recovery times for other grid impacts and other studies (Cannon et al., 2013). This scaling is easily adjustable and could be refined if future work were to indicate that these recovery times were not optimal for the analysis.

3. Construction of Power Grid Impact Scenarios

To quantify the global impact of a major space weather event, it is useful to consider the likely sequence of events that may occur during a 1-in-10-, 1-in-30-, and 1-in-100-year events. Candidate scenarios can be based around the March 1989 (1-in-30), Carrington (1-in-100), and October 2003 (1-in-10) events, as we now describe. This order reflects the logical process through which we developed and normalized the scenarios, with the 1-in-100-year scenario building on the 1-in-30-year scenario, while the 1-in-10-year scenario is independent of the other two. In particular, we begin with the 1989 event as this is, to date, the one which had the largest documented impact in the modern era. We note that following initial development, these scenarios were used as the basis for the UK-focussed study performed by Oughton et al. (2018).

3.1. The 1-in-30-Year Event

This scenario is derived from the observations of the great geomagnetic storm of 13–14 March 1989, shown in Figure 1a. Substorms were identified by taking the 31-min running median of 1-min resolution *AE* index data and then picking relevant maximum and minima by automated analysis. The *AE* index is shown in Figure 1. The initial impact longitude is assumed to be at 2.5 hr local time, reflecting experience from the 1989 storm where major grid impacts in Canada and the United Kingdom occurred during this event (but on different days). This initial impact longitude is used in all three scenarios. The qualitative intensity of each substorm is defined as moderate, high, intense, and very intense according to the definitions given in Table 1. Over a 2-week period of intense space weather centered on this storm, 85 substorms were calculated to have occurred. Supporting information Table S1 shows a subset of these substorms: those occurring during periods when geomagnetic activity reached or exceeded G1 intensity. Note that here we also identify secondary impact areas for the intense and very intense events, allowing for the possibility of a spread in impact longitude (and perhaps also a spread to lower latitudes).

3.2. The 1-in-100-Year Event

This scenario builds a simulated substorm sequence for a Carrington-class event. It is derived from the observations of the great geomagnetic storm of March 1989; it takes the substorm sequence from that event and replicates it twice so that we have two sets of substorms matching the two geomagnetic storm periods noted in Balfour Stewart's, paper on the Carrington event (Stewart, 1861). Thus, where a substorm was observed in 1989 at time Δt relative to the sudden storm commencement (SSC) that started the 1989 event, we replicate it twice in the 1-in-100-year scenario: (a) first at time Δt relative to the first SSC reported by Balfour Stewart and (b) second at time Δt relative to the second SSC reported by Balfour Stewart. In addition to this mapping in time, the intensity of all substorms in data set (b) is increased by a factor of 1.44 to reflect the higher intensity of the Carrington storm; this factor of increase represents the relative storm intensities as estimated from the *Dst* index: -589 measured in 1989 and -850 estimated for the second storm in 1859 (Siscoe et al., 2006). Thus, the scenario identifies a long sequence of bursts of activity (substorms) that may be taken as indicative of a Carrington-class event and includes estimates of where on Earth these would have had their prime impact. The simulated sequence consists of 127 substorms and is shown in Figure 1b. Supporting information Table S2 shows the results of this analysis for the high, intense, and very intense strength substorms.

3.3. The 1-in-10-Year Event

The 1-in-10-year event scenario builds on the substorm sequence derived from observations of the Halloween geomagnetic storm of October 2003. But to ensure consistent scaling with the two scenarios above, we adjusted the 2003 *AE* data downward by a factor of 0.62. This factor reflects the lower intensity of the 2003 storm as estimated from the *Dst* index: -589 measured at 14 March 1989 01:00 UT and -383 measured at 30 October 2003 22:00 UT. It is applied so that the peaks of smoothed *AE* adjacent to the times of minimum *Dst* (2011 at 14 March 1989 02:05 UT and 2113 at 30 October 2003 19:59 UT) are proportionally scaled. Having made this adjustment, the methodology is the same as for the previous scenario and the substorm time series is shown in Figure 1c. Supporting information Table S3 summarizes the resulting set of substorm occurrence, duration, severity, impact longitude, and primary target region. Note that only high, intense, and very intense substorms are listed.

4. Economic Analysis: Proposed Methodology and Illustrative Examples

4.1. Methodology

The next step in the analysis is to develop a model of the economic impact. Granularly capturing the various dimensions of economic impact is challenging, but we attempt it by using a combination of reduced form information on grid resilience for points (ii) and (iii) listed in section 1 and detailed spatiotemporal information on blackouts and Value-of-Lost-Load (VoLL) estimates at location for points (i) and (iv). Initially, this requires an approach to determine the economic impact of a single substorm of given duration and intensity, at a particular location on the globe. In addition to the different impact scenarios, we have also considered three different recovery periods, described as follows: (i) immediate recovery, defined as recovery immediately after the duration of occurrence of each substorm; (ii) no recovery, defined as zero recovery before

Table 3

Economic Costs (Median Estimates) of Space Weather (in Millions of Euros as of 27 August 2016) for the Only European Substorm (#21) in the 1-in-10-Year Scenario Under Different Forecast and Recovery Assumptions

| Total costs (EUR m) | Immediate recovery | No recovery | Linear recovery |
|---------------------|--------------------|-------------|-----------------|
| No forecast | ME 12.8 | ME 668 | ME 334 |
| Current forecast | ME 12.8 | ME 334 | ME 170 |
| Improved forecast | ME 0.00 | ME 0.00 | ME 0.00 |

Note. As described in the text, *immediate recovery* assumes that the disruption, if present, lasts for the duration of the substorm. *No recovery* assumes that there is full disruption until the end of the recovery period (e.g., 24 hr for western Europe in the current forecast conditions). *Linear recovery* assumes that the impact reduces linearly over the disruption duration; mathematically, this is half of the no recovery impact.

the end of the specific disruption period indicated in the impact tables shown in Table 3; and (iii) linear recovery, defined as uniform recovery from the end of each substorm occurrence to the end of the recovery period indicated in the impact tables shown in Table 2. Although other non-linear recovery rules could have been used to characterize the power system behavior between the immediate and no recovery case, a simple linear recovery rule provides a reasonable benchmark for intermediate forms of system resilience. Resilience can be inherent (e.g., good system design including the design of physical infrastructure and capabilities to reallocate resources and adjust to the conditions) or adaptive (e.g., extra ingenuity/effort exerted in crisis situations—in which case nowcasting can play a key role), and in the context of electricity disruptions resilience can take the form of lower-energy utilization per unit of output, fuel substitution, use of alternative generation sources, production rescheduling, etc. (see Rose et al., 2007). Some studies show that direct business resili-

ence is quite high and can result in damage estimates considerably lower than when resilience is ignored (e.g., Rose & Liao, 2005). The immediate recovery assumption can be thought as a proxy for a situation where both adaptive and inherent resilience are fully at play.

To quantify the economic impact itself, we focus on VoLL as a loss metric, quantifying both direct economic losses, such as production losses in different industries and indirect costs resulting from business interruption and opportunity costs from power outage (Coll-Mayor et al., 2012; de Nooij et al., 2007; Leahy & Tol, 2011; Tol, 2007). The empirical literature shows considerable variations in VoLL estimates, due to the highly skewed distribution of values from households to different industry sectors and the different estimation methodologies that can be used. As VoLL is not traded, it must be estimated either with a structural model (production-function approach) or by eliciting market participants' preferences via empirical evidence on consumer choices during power outages (revealed preference model) or questionnaires and contingent valuation surveys (stated preference models). Given our interest in forecasting, we find the last mentioned approach suitable for our analysis. Willingness-to-pay to avoid an outage and willingness-to-accept payment for an outage (Lehtonen & Lemstrom, 1995) are usually used to estimate consumers' VoLL. We acknowledge the disparity of results on willingness-to-pay/willingness-to-accept available in the literature, and therefore, our analysis is based on a range of possible VoLL estimates but is ultimately calibrated to produce median estimates consistent with the European Blackout simulator for UK and continental European exposures. The simulator is presented in Schmidthaler and Reichl (2016); see also discussions in the Royal Academy of Engineering study on electricity shortfalls (Royal Academy of Engineering, 2014) and Schmidthaler et al. (2015). The blackout simulator is used to quantify each substorm's direct economic cost at location. Residual, longer-term power outage or reduced system capacity are not considered in the estimates. As such, the latter can be interpreted as a lower bound for the economic losses associated with the impact table (Table 2). In this paper, the occurrence of direct power outage not recovered within 48 hr is restricted to the case of low-resilience locations affected by the very intense substorm #41 (see Table 2). In those instances, we extrapolate linearly the direct economic costs pertaining to the relevant areas.

To provide an assessment of international spillover, we use IO methodology (e.g., Haines et al., 2005; Miller & Blair, 2009), aggregating the cross-sectoral international impact of European power outages originating during the different substorms illustrated above (see the supporting information for further details with reference to Haines Yacov & Jiang, 2001; Leontief, 1951; Santos & Haines, 2004). In line with the existing literature, we rely on the 2011 Multi-Regional Input-Output table sourced from the World Input-Output Database. The IO methodology is well known to exaggerate indirect losses as it allows for unidirectional impacts, while the combination of partial and general equilibrium effects is more complex, in particular, due to the resilience of a system. In line with our above discussion on the concept of resilience, the existing literature suggests that damage reduction can be considerable (e.g., Rose & Liao, 2005), but on the other hand, indirect (general equilibrium) costs can raise costs significantly (e.g., Rose & Liao, 2005). Our application of IO analysis tries to capture some of these effects in reduced form and conservatively, providing indirect costs that are on average 30% lower than application of the standard model.

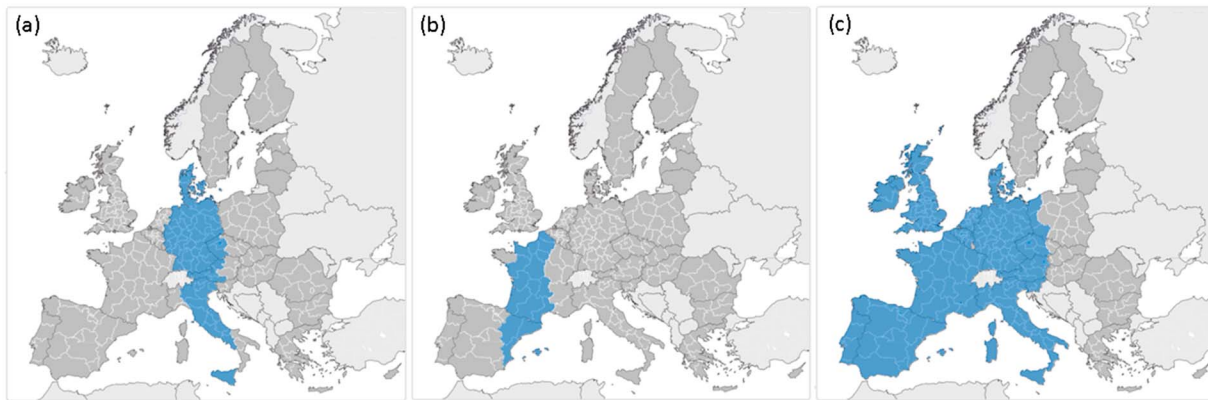


Figure 2. (a) Impact footprint of substorm 21 in the 1-in-10-year scenario. (b) Impact footprint of substorm 28 in the 1-in-30-year scenario. (c) Impact footprint of substorm 41 in the 1-in-30-year scenario. Figures are prepared using www.blackout-simulator.com.

4.2. An Individual Substorm

To illustrate the proposed approach, here we consider the impact of a single *high-intensity* substorm affecting western Europe (excluding Ireland and the United Kingdom) and Scandinavia for 1 hr and 9 min (substorm #21 in the 1-in-10-year scenario presented in section 4.3 and supporting information Table S3; the geographic footprint in continental Europe is shown in Figure 2a). We estimate the economic costs by allowing for the low and high resilience of the two geographic areas. Specifically, in this model Scandinavia experiences no impact irrespective of forecast. Western Europe experiences either no impact (improved forecast) or a limited power outage (2%) recovered in 48 hr (no forecast) or 24 hr (current forecast). This leads to the results reported in Table 3 for different recovery and forecast assumptions summarized in Table 2, modulated by the recovery profile. Under current forecast conditions and linear recovery, an estimated economic impact of €170 million is found.

It is instructive to break down these losses into different sectors. This is shown in Table 4. Note that we aggregate sectors in line with the classification used in the European blackout simulator (Schmidthaler & Reichl, 2016). With western Europe and Scandinavia being the focus of the event, it is manufacturing that experiences the most significant losses.

Turning to international spillover costs, these are reported in Table 5, again for different recovery and forecast assumptions. For current forecast conditions and linear recovery, this is calculated to be €22 to €32 billion. Table 5 demonstrates the sensitivity of this calculation to the initial cost calculation in Table 3. In the case of no forecast and no recovery until the end of the specified period after the substorm, the international spillover estimate is €359–506 billion. On the other hand, if the forecast quality is sufficient to ensure no direct impact, then evidently, there would be no indirect impact either.

4.3. Toward a Comprehensive Cost Model

The next level of complexity is to consider multiple substorms. To illustrate this, we examine the 1-in-30-year scenario and consider substorms #28 and #41 (see supporting information Table S1). Substorm #28 was a high-intensity event, with a geographic footprint shown in Figure 2b, which started at 00:35 on day 1 and had a duration of 2 hr 10 min. It was followed by event #41, a very intense substorm, which started at 01:05 on day 2 and had a duration of 2 hr 35 min. This substorm is modeled to have a very large geographic footprint as shown in Figure 2c. Here we will simply treat the substorms independently: No overlapping is assumed for the recovery periods pertaining to the two different substorms. Also, no recovery feedback effects from previous substorm are assumed in our analysis.

The aggregate costs of the two substorms on Europe alone are reported in Table 6. The numbers are considerably larger than in the previous scenario: For the current forecast/linear recovery case, the direct cost is estimated to be €9,340 million. This is driven by the impact of the very intense substorm on a low-resilience grid, where for the current forecast, we model the impact as being of much longer duration. For example, the system capacity is reduced by 4% and recovered in 5 months.

Table 4
Economic Costs (Million EUR) to Different Sectors Resulting From the Substorm Described in Table 3

| Sector | No forecast | | | Current forecast | | | Improved forecast | | |
|--|--------------------|------------------------|-----------------|--------------------|------------------------|-----------------|--------------------|------------------------|-----------------|
| | Immediate recovery | Recovery after X hours | Linear recovery | Immediate recovery | Recovery after X hours | Linear recovery | Immediate recovery | Recovery after X hours | Linear recovery |
| Agriculture, forestry, and fishing | 0.18 | 13.11 | 6.55 | 0.18 | 6.55 | 3.41 | 0.00 | 0.00 | 0.00 |
| Mining and quarrying/electricity, gas, steam, and air conditioning supply/water supply/sewerage/waste management and remediation activities | 0.54 | 7.13 | 3.56 | 0.54 | 3.56 | 1.78 | 0.00 | 0.00 | 0.00 |
| Manufacturing | 7.16 | 296.83 | 148.42 | 7.16 | 148.42 | 74.63 | 0.00 | 0.00 | 0.00 |
| Construction | 0.10 | 15.13 | 7.56 | 0.10 | 7.56 | 3.99 | 0.00 | 0.00 | 0.00 |
| Wholesale and retail trade/repair of motor vehicles and motorcycles/transporting and storage, accommodation, and food service activities | 0.63 | 44.29 | 22.14 | 0.63 | 22.14 | 10.39 | 0.00 | 0.00 | 0.00 |
| Information and communication | 0.36 | 14.35 | 7.17 | 0.36 | 7.17 | 3.59 | 0.00 | 0.00 | 0.00 |
| Financial and insurance activities | 0.12 | 17.97 | 8.99 | 0.12 | 8.99 | 4.61 | 0.00 | 0.00 | 0.00 |
| Real estate activities/professional, scientific, and technical activities/administrative and support service activities | 0.60 | 93.48 | 46.74 | 0.60 | 46.74 | 25.15 | 0.00 | 0.00 | 0.00 |
| Public administration and defense/compulsory social security/education/human health and social work activities/arts, entertainment, and recreation/other services activities | 1.16 | 84.21 | 42.11 | 1.16 | 42.11 | 22.25 | 0.00 | 0.00 | 0.00 |
| Households | 1.94 | 81.26 | 40.63 | 1.94 | 40.63 | 20.31 | 0.00 | 0.00 | 0.00 |

Note. Each column sums to the relevant entry in Table 3.

Table 7 reports the results broken down by sector. As before, manufacturing accounts for the most significant losses, but for this severity of event households now experience the second highest losses. Using IO analysis, we quantify the indirect economic costs of the two substorms by looking at cross-country and cross-sectoral spillovers. The economic costs of the two substorms are reported in Table 8 and illustrate a significant difference between the different types of forecast. For the current forecast/linear recovery case, the estimated indirect cost impact is €787–1,108 billion. This represents global losses. The complete loss of forecast capability results in a tenfold increase in costs across all sectors.

5. Discussion and Conclusions

Although the proposed approach necessarily leads to very detailed scenarios, particularly in the most severe and long-lived events, we argue that such an approach is necessary to fully understand the complex impacts of space weather. The approach is deliberately conservative, in the sense that it is based around elemental events that are limited in spatial footprint and duration, but nevertheless, this provides a way to

Table 5
Range Estimates of Total International Spillovers Across All Sectors (in Billion Euros as of 27 August 2016) for a European Substorm of High Strength Under Different Forecast and Recovery Assumptions

| Total costs (EUR Bn) | Immediate recovery | No recovery | Linear recovery |
|----------------------|--------------------|--------------------|-------------------|
| No forecast | Bn € 0.18–0.25 | Bn € 359.26–506.00 | Bn € 89.81–126.50 |
| Current forecast | Bn € 0.18–0.25 | Bn € 89.81–126.50 | Bn € 22.46–31.64 |
| Improved forecast | Bn € 0.00–0.00 | Bn € 0.00–0.00 | Bn € 0.00–0.00 |

Table 6

Economic Costs (Median Estimates) of Space Weather (in Millions of Euros as of 27 August 2016) for the Two European Substorms Characterizing the 1-in-30-Year Scenario Under Different Forecast and Recovery Assumptions, in a Similar Format to Table 3

| Total costs (EUR m) | Immediate recovery | No recovery | Linear recovery |
|---------------------|--------------------|-------------|-----------------|
| No forecast | ME 1,570 | ME 55,500 | ME 27,900 |
| Current forecast | ME 1,510 | ME 18,300 | ME 9,340 |
| Improved forecast | ME 635 | ME 7,340 | ME 3,700 |

comprehensively estimate and understand the impact of a complex space weather event. It also provides a pathway to examine the full range of space weather economic impacts, particularly from smaller events that may occur more frequently. This is related to a growing realization that vulnerability may arise not simply due to rare but severe events but also due to continuing degradation as a consequence of many smaller impacts (Schrijver et al., 2015). The analysis of section 4.2 shows that even isolated substorms causing a limited outage can have a significant economic impact. In the case of two substorms over western Europe and for current forecast/linear recovery

conditions, the direct cost is estimated to be €9,340 million, with an estimated international spillover costs in the range of €787–1,108 billion. We have also attempted to quantify the impact of improved forecasting and adjustments to the impact recovery footprint or time scale can have a significant impact. For example, in the two substorm case with linear recovery, moving from the current to the improved forecasting scenario (approximately halving the physical impact footprint) reduces the economic impact by a factor of ~3 to €3.7 billion. It also reduces the spillover cost by a factor of 4. The development of improved situational knowledge is therefore likely to have a very significant cost/benefit ratio.

In making policy decisions, these benefits are tensioned against the cost of developing and operating an improved forecast system. Such an analysis is beyond the scope of the present work as it depends on the unique circumstances of each entity tasked with mitigating space weather risk. However, we offer the following observations. The decision to pursue such a mission would depend not only on power grid impact but also on all other sectors that are affected by space weather. Furthermore, each sector has its own requirements for the time scale on which resilience is formally justified (in several cases this may be at the 1-in-100 or 1-in-200-year level). A recent ESA study provides an estimated cost of €502 m over 2016–2032 to enable an improved forecast system (ESA, 2016).

Table 7

Breakdown of the Results of Table 6 by Sectoral Groups (Million EUR)

| Sector | No forecast | | | Current forecast | | | Improved Forecast | | |
|--|--------------------|------------------------|-----------------|--------------------|------------------------|-----------------|--------------------|------------------------|-----------------|
| | Immediate recovery | Recovery after X hours | Linear recovery | Immediate recovery | Recovery after X hours | Linear recovery | Immediate recovery | Recovery after X hours | Linear recovery |
| Agriculture, forestry, and fishing | 37.00 | 1,796.12 | 909.82 | 36.26 | 596.50 | 310.37 | 14.86 | 237.83 | 122.60 |
| Mining and quarrying/electricity, gas, steam, and air conditioning supply/water supply/sewerage/waste | 25.12 | 578.74 | 289.37 | 23.61 | 189.17 | 94.59 | 10.32 | 76.52 | 38.26 |
| Manufacturing | 666.52 | 20,929.86 | 10,492.63 | 646.03 | 6,918.31 | 3,487.32 | 269.67 | 2,772.53 | 1,385.73 |
| Construction | 18.29 | 1,429.33 | 726.37 | 17.36 | 469.40 | 247.17 | 7.46 | 189.38 | 95.05 |
| Wholesale and retail trade/repair of motor vehicles and motorcycles/transporting and storage | 103.69 | 3,863.88 | 1,892.99 | 99.56 | 1,273.92 | 596.21 | 42.11 | 509.44 | 235.83 |
| Information and communication | 59.66 | 1,385.77 | 692.89 | 56.78 | 455.70 | 227.85 | 24.29 | 182.84 | 91.42 |
| Financial and insurance activities | 24.09 | 2,081.08 | 1,046.04 | 22.82 | 682.67 | 345.43 | 9.84 | 273.07 | 132.78 |
| Real estate activities/professional, scientific, and technical activities/administrative and support service | 82.47 | 7,540.26 | 3,864.70 | 79.97 | 2,494.47 | 1,339.90 | 33.32 | 994.66 | 523.50 |
| Public administration and defense/ compulsory social security/ education/human health and social work activities/arts, entertainment, and recreation/other | 157.75 | 7,689.28 | 3,914.81 | 151.02 | 2,532.33 | 1,339.94 | 64.15 | 1,019.41 | 525.33 |
| Households | 392.83 | 8,213.50 | 4,106.75 | 378.88 | 2,710.54 | 1,355.27 | 159.28 | 1,087.32 | 546.84 |

Note. Each column sums to the relevant entry in Table 6.

Table 8*Economic Costs (Median Estimates) of Space Weather (in Billion Euros as of 27 August 2016) for European Substorms #28 and #41 Under Different Forecast and Recovery Assumptions*

| Total costs (EUR Bn) | Immediate recovery | No recovery | Linear recovery |
|----------------------|--------------------|--------------------|------------------|
| No forecast | Bn € 481–677 | Bn € 23,483–33,074 | Bn € 5,871–8,269 |
| Current forecast | Bn € 51–71 | Bn € 13,551–19,086 | Bn € 787–1,108 |
| Improved forecast | Bn € 46–65 | Bn € 690–971 | Bn € 193–272 |

Note. This represents all losses including those arising globally as a consequence of the international spillover.

It is evident that the multiplicative effects of many such events during a prolonged Carrington-type event have the potential to be extremely severe. However, the calculation of economic impact for the whole scenario cannot yet be performed with confidence for several reasons, and this indicates areas that require immediate further investigation.

- The analysis can only be performed with confidence if reliable data on power grid infrastructure, and hence, direct economic losses of sufficient quality and fidelity are available. While the data for western Europe are relatively mature, we were unable to acquire the necessary data from other regions of the world to attempt a more comprehensive analysis.
- The recovery scenarios used here are relatively simple and also can be adjusted or made more complex in response to improved knowledge about likely impact. In particular, the presence of other on-going space weather effects could impact the recovery and/or the operation of power networks. For example, it has recently been recognized by the UK government that space weather can also impact the power grid via Global Navigation Satellite Systems (London Economics, 2017, p. 51).
- Although the scenarios are derived from real observations, they are only representative. For example, shifting the onset time of each event by 6 hr would change the calculation significantly, since events that might happen in the United States would instead have their footprint over the Pacific Ocean. In the case of the 1-in-100-year scenario, the construction of the scenario is such that many of the most severe impacts occur over North America. This arises because we have used timings from the 1859 Carrington event and is consistent with historical records from 1859 that report strong effects over the continental United States such as disruption of telegraph systems and spectacular auroral displays, (e.g., see the collection of papers edited by Clauer & Siscoe, 2006). For the 1-in-10- and 1-in-30-year scenarios, the effects are even more regionally located, and so it should be understood that a full analysis requires a Monte Carlo-type analysis where the timing, ordering, and intensity of the substorms are changed both systematically and randomly.
- Finally, the total cost of all these events is unlikely to combine linearly, and indeed, it is not yet known how the knock-on effects should be treated. For example, a power outage is likely to cause knock-on effects in adjacent regions not captured here; it is not yet clear how this should modify the impact calculation. This becomes increasingly important as the complexity and duration of the scenario increases, evidently most so in the 1-in-100-year scenario.

Although construction of the total economic cost of a particular scenario should therefore be approached extremely carefully (and we do not attempt such a calculation here), investigation of these aspects building on the framework approach presented here will enable a more robust assessment of space weather economic impact and facilitate evidence-based policy decisions. Furthermore, we anticipate that this framework approach can also be applied to other space weather impacts in the future (e.g., aviation and Global Navigation Satellite Systems).

Acknowledgments

Data are publicly available from the World Data Center for Geomagnetism, Kyoto (<http://wdc.kugi.kyoto-u.ac.jp/aedir/>), the International Service on Rapid Magnetic Variations (<http://www.obsebre.es/en/rapid>), the Blackout Simulator (<http://www.blackout-simulator.com>), and the World Input Output Database (<http://www.wiod.org/home>). This work was funded by the UK Space Agency International Partnership Space Programme (collaboration agreement L2796 and NERC grant NE/P017142/1). E. B. acknowledges useful discussions with Richard Green and Malcolm Kemp/Nematrian. The authors thank the reviewers for helpful and constructive comments during the review process.

References

- ABT Associates (2017). Social and economic impacts of space weather in the United States (Rep). National Oceanic and Atmospheric Administration. Retrieved from https://www.weather.gov/news/171212_spaceweatherreport
- Anderson, C. W., Santos, J. R., & Haines, Y. Y. (2007). A risk-based input-output methodology for measuring the effects of the August 2003 northeast blackout. *Economic Systems Research*, 19(2), 183–204. <https://doi.org/10.1080/09535310701330233>
- Bartels, J., Heck, N. H., & Johnston, H. F. (1939). The three-hour-range index measuring geomagnetic activity. *Journal of Geophysical Research*, 44(4), 411–454.
- Beamish, D., Clark, T. D. G., Clarke, E., & Thomson, A. W. P. (2002). Geomagnetically induced currents in the UK: Geomagnetic variations and surface electric fields. *Journal of Atmospheric and Solar: Terrestrial Physics*, 64(16), 1779–1792. [https://doi.org/10.1016/S1364-6826\(02\)00127-X](https://doi.org/10.1016/S1364-6826(02)00127-X)

- Bolduc, L. (2002). GIC observations and studies in the Hydro-Quebec power system. *Journal of Atmospheric and Solar: Terrestrial Physics*, 64(16), 1793–1802.
- Cabinet Office (2015). Space weather preparedness strategy *Rep.*, BIS/15/457 UK Government, Department for Business Innovation and Skills London.
- Cannon, P., Angling, M., Barclay, L., Curry, C., Dyer, C., Edwards, R., et al. (2013). Extreme space weather: Impacts on engineered systems and infrastructure *Rep.*, ISBN 1–903496–95–0, Royal Academy of Engineering, London.
- Carter, B. A., Yizengaw, E., Pradipta, R., Halford, A. J., Norman, R., & Zhang, K. (2015). Interplanetary shocks and the resulting geomagnetically induced currents at the equator. *Geophysical Research Letters*, 42, 6554–6559. <https://doi.org/10.1002/2015GL065060>
- Clauser, R. C., & Siscoe, G. (2006). The great historical geomagnetic storm of 1859: A modern look. *Advances in Space Research*, 38(2), 117–118. <https://doi.org/10.1016/j.asr.2006.09.001>
- Coll-Mayor, D., Pardo, J., & Perez-Donsion, M. (2012). Methodology based on the value of lost load for evaluating economical losses due to disturbances in the power quality. *Energy Policy*, 50, 407–418. <https://doi.org/10.1016/j.enpol.2012.07.036>
- Davis, T. N., & Sugiura, M. (1966). Auroral electrojet activity index AE and its universal time variations. *Journal of Geophysical Research*, 71(3), 785–801. <https://doi.org/10.1029/JZ071i003p00785>
- Eastwood, J. P., Biffs, E., Hapgood, M. A., Green, L., Bisi, M. M., Bentley, R. D., et al. (2017). The economic impact of space weather: Where do we stand? *Risk Analysis*, 37(2), 206–218. <https://doi.org/10.1111/risa.12765>
- Eastwood, J. P., Kataria, D. O., McInnes, C. R., Barnes, N. C., & Mulligan, P. (2015). Sunjammer. *Weather*, 70(1), 27–30. <https://doi.org/10.1002/wea.2438>
- Eastwood, J. P., Nakamura, R., Turc, L., Mejnertsen, L., & Hesse, M. (2017). The scientific foundations of forecasting magnetospheric space weather. *Space Science Reviews*, 212(3), 1221–1252. <https://doi.org/10.1007/s11214-017-0399-8>
- Erinmez, I. A., Kappenman, J. G., & Radasky, W. A. (2002). Management of the geomagnetically induced current risks on the national grid company's electric power transmission system. *Journal of Atmospheric and Solar - Terrestrial Physics*, 64(5–6), 743–756. [https://doi.org/10.1016/s1364-6826\(02\)00036-6](https://doi.org/10.1016/s1364-6826(02)00036-6)
- European Space Agency (2016). SWE cost benefit analysis *Rep.*, Paris.
- Fiori, R. A. D., Boteler, D. H., & Gillies, D. M. (2014). Assessment of GIC risk due to geomagnetic sudden commencements and identification of the current systems responsible. *Space Weather*, 12, 76–91. <https://doi.org/10.1002/2013SW000967>
- Forbes, K. F., & St Cyr, O. C. (2012). Did geomagnetic activity challenge electric power reliability during solar cycle 23? Evidence from the PJM regional transmission organization in North America. *Space Weather-the International Journal of Research and Applications*, 10. <https://doi.org/10.1029/2011SW000752>
- Gaunt, C. T. (2014). Reducing uncertainty—Responses for electricity utilities to severe solar storms. *Journal of Space Weather and Space Climate*, 4, A01.
- Gaunt, C. T., & Coetzee, G. (2007). Transformer failures in regions incorrectly considered to have low GIC-risk. *IEEE Lausanne Powertech*, 1–5, 807–812. <https://doi.org/10.1109/pct.2007.4538419>
- Haimes, Y. Y., Horowitz, B. M., Lambert, J. H., Santos, J. R., Lian, C., & Crowther, K. G. (2005). Inoperability input-output model for interdependent infrastructure sectors. I: Theory and Methodology. *Journal of Infrastructure Systems*, 11(2), 67–79. [https://doi.org/10.1061/\(ASCE\)1076-0342\(2005\)11:2\(67\)](https://doi.org/10.1061/(ASCE)1076-0342(2005)11:2(67))
- Haimes Yacov, Y., & Jiang, P. (2001). Leontief-based model of risk in complex interconnected infrastructures. *Journal of Infrastructure Systems*, 7(1), 1–12. [https://doi.org/10.1061/\(ASCE\)1076-0342\(2001\)7\(1\)](https://doi.org/10.1061/(ASCE)1076-0342(2001)7(1))
- Hapgood, M. (2010). Space weather: Its impact on Earth and implications for business *Rep.*, Lloyd's, London.
- Henry, D., & Emmanuel Ramirez-Marquez, J. (2012). Generic metrics and quantitative approaches for system resilience as a function of time. *Reliability Engineering & System Safety*, 99, 114–122. <https://doi.org/10.1016/j.res.2011.09.002>
- Howell, L. (2013). In W. E. Forum (Ed.), *Global risks 2013 eighth edition*. Switzerland: World Economic Forum.
- Juusola, L., Viljanen, A., van de Kamp, M., Tanskanen, E. I., Vanhamaki, H., Partamies, N., & Kauristie, K. (2015). High-latitude ionospheric equivalent currents during strong space storms: Regional perspective. *Space Weather-the International Journal of Research and Applications*, 13, 49–60. <https://doi.org/10.1002/2014sw001139>
- Kappenman, J. G. (2003). Storm sudden commencement events and the associated geomagnetically induced current risks to ground-based systems at low-latitude and midlatitude locations. *Space Weather*, 1(3), 1016. <https://doi.org/10.1029/2003SW000009>
- Kappenman, J. (2010). Geomagnetic storms and their impact on the US power grid *Rep.*, Metatech Corp.
- Lanzerotti, L. J. (1992). Comment on “Great magnetic storms” by Tsurutani et al. *Geophysical Research Letters*, 19(19), 1991–1992. <https://doi.org/10.1029/92GL02238>
- Leahy, E., & Tol, R. S. J. (2011). An estimate of the value of lost load for Ireland. *Energy Policy*, 39(3), 1514–1520. <https://doi.org/10.1016/j.enpol.2010.12.025>
- Lehtonen, M., and B. Lemstrom (1995). Comparison of the methods for assessing the customers' outage costs, paper presented at Energy Management and Power Delivery, 1995. Proceedings of EMPD '95., 1995 International Conference on, 21–23 Nov 1995.
- Leontief, W. W. (1951). Input-output economics. *Scientific American*, 185(4), 15–21.
- Lloyd's (2013). Solar storm risk to the North American electric grid *Rep.*, Lloyd's.
- London Economics (2017). The economic impact on the UK of a disruption to GNSS *Rep.*, London Economics, London.
- Lotz, S. I., & Cilliers, P. J. (2015). A solar wind-based model of geomagnetic field fluctuations at a mid-latitude station. *Advances in Space Research*, 55(1), 220–230. <https://doi.org/10.1016/j.asr.2014.09.014>
- Marshall, R. A., Dalzell, M., Waters, C. L., Goldthorpe, P., & Smith, E. A. (2012). Geomagnetically induced currents in the New Zealand power network. *Space Weather*, 10, S08003. <https://doi.org/10.1029/2012SW000806>
- Matandirotya, E., Cilliers, P. J., & Van Zyl, R. R. (2015). Modeling geomagnetically induced currents in the South African power transmission network using the finite element method. *Space Weather-the International Journal of Research and Applications*, 13, 185–195. <https://doi.org/10.1002/2014sw001135>
- Miller, R. E., & Blair, P. D. (2009). *Input-output analysis: Foundations and extensions*. Cambridge, GBR: Cambridge University Press.
- Natural Environment Research Council (2010). High-impact, low frequency event risk to the North American power system *Rep.*, North America Electric Reliability Cooperation.
- Natural Environment Research Council (2012). Effects of geomagnetic disturbances on the bulk power system *Rep.*, North America Electric Reliability Corporation.
- Ngwira, C. M., Pulkkinen, A., Leila Mays, M., Kuznetsova, M. M., Galvin, A. B., Simunac, K., et al. (2013). Simulation of the 23 July 2012 extreme space weather event: What if this extremely rare CME was Earth directed? *Space Weather*, 11, 671–679. <https://doi.org/10.1002/2013SW000990>

- de Nooij, M., Koopmans, C., & Bijvoet, C. (2007). The value of supply security: The costs of power interruptions: Economic input for damage reduction and investment in networks. *Energy Economics*, 29(2), 277–295. <https://doi.org/10.1016/j.eneco.2006.05.022>
- Organisation for Economic Co-operation and Development (2011). Future global shocks. Improving risk governance *Rep.*, OECD.
- Oughton, E. J. (2018). The Economic Impact of Critical National Infrastructure Failure Due to Space Weather. *Oxford Research Encyclopedia of Natural Hazard Science*. <https://doi.org/10.1093/acrefore/9780199389407.013.315>
- Oughton, E. J., Copic J., Skelton A., Kesaite V., Yeo J. Z., Ruffle S. J., et al. (2016). Helios solar storm scenario *Rep.*, Centre for Risk Studies, University of Cambridge, Cambridge.
- Oughton, E. J., Hapgood, M., Richardson, G. S., Beggan, C. D., Thomson, A. W. P., Gibbs, M., et al. (2018). A Risk Assessment Framework for the Socioeconomic Impacts of Electricity Transmission Infrastructure Failure Due to Space Weather: An Application to the United Kingdom. *Risk Analysis*. <https://doi.org/10.1111/risa.13229>
- Oughton, E. J., Skelton, A., Horne, R. B., Thomson, A. W. P., & Gaunt, C. T. (2017). Quantifying the daily economic impact of extreme space weather due to failure in electricity transmission infrastructure. *Space Weather*, 15, 65–83. <https://doi.org/10.1002/2016SW001491>
- Pant, R., Barker, K., Ramirez-Marquez, J. E., & Rocco, C. M. (2014). Stochastic measures of resilience and their application to container terminals. *Computers & Industrial Engineering*, 70, 183–194. <https://doi.org/10.1016/j.cie.2014.01.017>
- Pirjola, R., Kauristie, K., Lappalainen, H., Viljanen, A., & Pulkkinen, A. (2005). Space weather risk. *Space Weather*, 3, S02A02. <https://doi.org/10.1029/2004SW000112>
- Pulkkinen, A., Bernabeu, E., Eichner, J., Viljanen, A., & Ngwira, C. (2015). Regional-scale high-latitude extreme geoelectric fields pertaining to geomagnetically induced currents. *Earth, Planets and Space*, 67(1), 1–8. <https://doi.org/10.1186/s40623-015-0255-6>
- Pulkkinen, A., Lindahl, S., Viljanen, A., & Pirjola, R. (2005). Geomagnetic storm of 29–31 October 2003: Geomagnetically induced currents and their relation to problems in the Swedish high-voltage power transmission system. *Space Weather*, 3, S08C03. <https://doi.org/10.1029/2004SW000123>
- Rose, A., & Liao, S.-Y. (2005). Modeling regional economic resilience to disasters: A computable general equilibrium analysis of water service disruptions*. *Journal of Regional Science*, 45(1), 75–112. <https://doi.org/10.1111/j.0022-4146.2005.00365.x>
- Rose, A., Olatosun, G., & Liao, S.-Y. (2007). Business interruption impacts of a terrorist attack on the electric power system of Los Angeles: Customer resilience to a total blackout. *Risk Analysis*, 27(3), 513–531. <https://doi.org/10.1111/j.1539-6924.2007.00912.x>
- Royal Academy of Engineering (2014). *Counting the cost: The economic and social costs of electricity shortfalls in the UK*. London: Royal Academy of Engineering.
- Santos, J. R., & Haines, Y. Y. (2004). Modeling the demand reduction input-output (I-O) inoperability due to terrorism of interconnected infrastructures*. *Risk Analysis*, 24(6), 1437–1451. <https://doi.org/10.1111/j.0272-4332.2004.00540.x>
- Schmidthaler, M., Cohen, J., Reichl, J., & Schmidinger, S. (2015). The effects of network regulation on electricity supply security: A European analysis. *Journal of Regulatory Economics*, 48(3), 285–316. <https://doi.org/10.1007/s11149-015-9277-z>
- Schmidthaler, M., & Reichl, J. (2016). Assessing the socio-economic effects of power outages ad hoc. *Computer Science - Research and Development*, 31(3), 157–161. <https://doi.org/10.1007/s00450-014-0281-9>
- Schrijver, C. J., Dobbins, R., Murtagh, W., & Petrinec, S. M. (2014). Assessing the impact of space weather on the electric power grid based on insurance claims for industrial electrical equipment. *Space Weather-the International Journal of Research and Applications*, 12, 487–498. <https://doi.org/10.1002/2014sw001066>
- Schrijver, C. J., Kauristie, K., Aylward, A. D., Denardini, C. M., Gibson, S. E., Glover, A., et al. (2015). Understanding space weather to shield society: A global road map for 2015–2025 commissioned by COSPAR and ILWS. *Advances in Space Research*, 55(12), 2745–2807. <https://doi.org/10.1016/j.asr.2015.03.023>
- Schrijver, C. J., & Mitchell, S. D. (2013). Disturbances in the US electric grid associated with geomagnetic activity. *Journal of Space Weather and Space Climate*, 3. <https://doi.org/10.1051/swsc/2013041>
- Schulte in den Bäumen, H., Moran, D., Lenzen, M., Cairns, I., & Steenge, A. (2014). How severe space weather can disrupt global supply chains. *Natural Hazards and Earth System Sciences*, 14(10), 2749–2759. <https://doi.org/10.5194/nhess-14-2749-2014>
- Showstack, R. (2011). Threat of severe space weather to the US electrical grid explored at conference. *Eos, Transactions American Geophysical Union*, 92, 374–375.
- Siscoe, G., Crooker, N. U., & Clauer, C. R. (2006). Dst of the Carrington storm of 1859. *Advances in Space Research*, 38(2), 173–179. <https://doi.org/10.1016/j.asr.2005.02.102>
- Smith, P. M. (1990). Effects of geomagnetic disturbances on the national grid system, Paper Presented at 25th Universities Power Engineering Conference, Robert Gordon's Institute of Technology, Robert Gordon's Institute of Technology, Aberdeen.
- Stewart, B. (1861). On the great magnetic disturbance which extended from August 28 to September 7, 1859, as recorded by photography at the Kew Observatory. *Philosophical Transactions of the Royal Society*, 151, 423–430. <https://doi.org/10.1098/rstl.1861.0023>
- Thomson, A. W. P., Dawson, E. B., & Reay, S. J. (2011). Quantifying extreme behavior in geomagnetic activity. *Space Weather-the International Journal of Research and Applications*, 9, 12. <https://doi.org/10.1029/2011sw000696>
- Thomson, A. W. P., McKay, A. J., Clarke, E., & Reay, S. J. (2005). Surface electric fields and geomagnetically induced currents in the Scottish Power grid during the 30 October 2003 geomagnetic storm. *Space Weather*, 3, S11002. <https://doi.org/10.1029/2005SW000156>
- Tol, R. S. J. (2007). The value of lost load *Rep.*, The Economic and Social Research Institute (ESRI), Dublin.
- Torta, J. M., Serrano, L., Regue, J. R., Sanchez, A. M., & Roldan, E. (2012). Geomagnetically induced currents in a power grid of northeastern Spain. *Space Weather-the International Journal of Research and Applications*, 10, 11. <https://doi.org/10.1029/2012sw000793>
- Trivedi, N. B., Vitorello, I., Kabata, W., Dutra, S. L. G., Padilha, A. L., Bologna, M. S., et al. (2007). Geomagnetically induced currents in an electric power transmission system at low latitudes in Brazil: A case study. *Space Weather-the International Journal of Research and Applications*, 5. <https://doi.org/10.1029/2006sw000282>
- US - Canada Power System Outage Task Force (2006). Final report on the implementation of the task force recommendations *Rep.*, Natural Resources Canada and US Department of Energy.
- Viljanen, A. (2011). European project to improve models of geomagnetically induced currents. *Space Weather*, 9, S07007. <https://doi.org/10.1029/2011SW000680>
- Viljanen, A., Pulkkinen, A., Pirjola, R., Pajunpaa, K., Posio, P., & Koistinen, A. (2006). Recordings of geomagnetically induced currents and a nowcasting service of the Finnish natural gas pipeline system. *Space Weather-the International Journal of Research and Applications*, 4. <https://doi.org/10.1029/2006sw000234>
- Villiers, J. S., Kosch, M., Yamazaki, Y., & Lotz, S. (2017). Influences of various magnetospheric and ionospheric current systems on geomagnetically induced currents around the world. *Space Weather*, 15, 403–417. <https://doi.org/10.1002/2016SW001566>
- Wang, K.-R., Lian-guang, L. I. U., & Yan, L. I. (2015). Preliminary analysis on the interplanetary cause of geomagnetically induced current and its effect on power systems. *Chinese Astronomy and Astrophysics*, 39(1), 78–88. <https://doi.org/10.1016/j.chinastron.2015.01.003>

- Watari, S. (2015). Estimation of geomagnetically induced currents based on the measurement data of a transformer in a Japanese power network and geoelectric field observations. *Earth, Planets and Space*, 67(1), 12. <https://doi.org/10.1186/s40623-015-0253-8>
- Wik, M., Pirjola, R., Lundstedt, H., Viljanen, A., Wintoft, P., & Pulkkinen, A. (2009). Space weather events in July 1982 and October 2003 and the effects of geomagnetically induced currents on Swedish technical systems. *Annales Geophysicae*, 27(4), 1775–1787.